Journal of *Marine Science and Engineering*

MDPI

Article

Palytoxin-Analogues Accumulation in Natural Mussel Banks during an *Ostreopsis* cf. *ovata* Bloom

Stefano Accoroni [1,2,*], Marika Ubaldi [1], Simone Bacchiocchi [2], Francesca Neri [1], Melania Siracusa [1,2], Maria Giovanna Buonomo [3], Alessandra Campanelli [4] and Cecilia Totti [1]

[1] Dipartimento di Scienze della Vita e dell'Ambiente, Università Politecnica delle Marche, Via Brecce Bianche, 60131 Ancona, Italy
[2] Istituto Zooprofilattico Sperimentale Umbria e Marche "Togo Rosati", Via G. Salvemini, 1, 06126 Perugia, Italy
[3] Istituto Zooprofilattico Sperimentale del Mezzogiorno, Via Salute, 2, 80055 Portici, Italy
[4] Consiglio Nazionale delle Ricerche, CNR-IRBIM, Largo Fiera della Pesca, 2, 60125 Ancona, Italy
* Correspondence: s.accoroni@univpm.it

Abstract: Intense blooms of the toxic dinoflagellate *Ostreopsis* producing palytoxin (PlTX) analogs, mainly ovatoxins (OVTXs), have been a recurrent phenomenon along several Mediterranean coasts. Although there is evidence of seafood contamination by these toxins, the dynamics of their bioaccumulation during *Ostreopsis* blooms is not yet clear. Toxin concentrations in wild mussels at two sites in the Conero Riviera, along the northern Adriatic Sea (Portonovo and Passetto), were analyzed from August to October 2021, throughout an *Ostreopsis* cf. *ovata* bloom, to investigate their relationships with the bloom pattern and abundances. Contaminated mussels showed the typical toxin profile dominated by OVTX-a and -b, with levels lower than the threshold considered unsafe for human consumption (30 µg PlTX-equivalent kg^{-1} soft tissue). The toxin content reached 36.4 µg PlTX kg^{-1} soft tissue only in a single sampling date. A clear correlation between the bioaccumulation of OVTXs in mussels and the abundance of *Ostreopsis* was observed. Our results highlighted, however, that bioaccumulation in the mussels is not affected merely by the abundance of toxic microalgae, since higher toxin levels were recorded at Portonovo, where the cell abundances were lower than at Passetto. The results from this study indicate that the Italian guidelines for the management of *Ostreopsis* blooms in bathing waters are also useful in managing the risks of human intoxication through ingestion, as mussel contamination was detected only during the alert phase (10,000–30,000 cells L^{-1}).

Keywords: harmful algae; toxicity; palytoxin; emerging toxins; toxic algae; benthic dinoflagellates

Citation: Accoroni, S.; Ubaldi, M.; Bacchiocchi, S.; Neri, F.; Siracusa, M.; Buonomo, M.G.; Campanelli, A.; Totti, C. Palytoxin-Analogues Accumulation in Natural Mussel Banks during an *Ostreopsis* cf. *ovata* Bloom. *J. Mar. Sci. Eng.* **2022**, *10*, 1402. https://doi.org/10.3390/jmse10101402

Academic Editor: Wang Fat Fred Lee

Received: 5 August 2022
Accepted: 26 September 2022
Published: 1 October 2022

1. Introduction

The genus *Ostreopsis* includes species of benthic dinoflagellates growing on a number of substrata, such as large-sized macroalgae, algal turfs, seagrasses, coral rubble, rocks, and sediments [1]. They are also found in plankton, in the form of aggregates floating at the sea surface, or freely swimming in the water column [2]. They show the highest diversity in tropical areas [3,4], where they reach maximum abundances of 10^5 cells g^{-1} fw [5–15]. Their presence in temperate latitudes is considered recent [16,17]. It is therefore remarkable that in temperate regions they can reach considerably higher abundances than in tropical regions (up to 10^6 cells g^{-1} fw [18,19]).

Several species of this genus produce toxins, mainly ovatoxins (OVTXs), belonging to the group of palytoxin (PlTX) analogs (Figure 1) [20–28]. In tropical areas, *Ostreopsis* (i.e., *O. siamensis*) is strongly suspected (although without confirmation) to be involved in some events of clupeotoxism. This intoxication is characterized by a symptomatology similar to that of ciguatera but with a much higher mortality rate, due to the consumption of contaminated crustaceans and finfish (Fam. Clupeidae) [29,30]. In temperate areas, such as the Mediterranean Sea, there are no reports of intoxications due to the ingestion of contaminated seafood [31]. At these latitudes, however, *Ostreopsis* blooms (mainly produced by *O.* cf. *ovata*)

cause problems related to human health, mostly due to the inhalation of seawater droplets containing aerosolized toxins and/or fragments of microalgal cells, or cutaneous contact with cells, causing mainly dermatitis and ocular irritation/conjunctivitis [32–34].

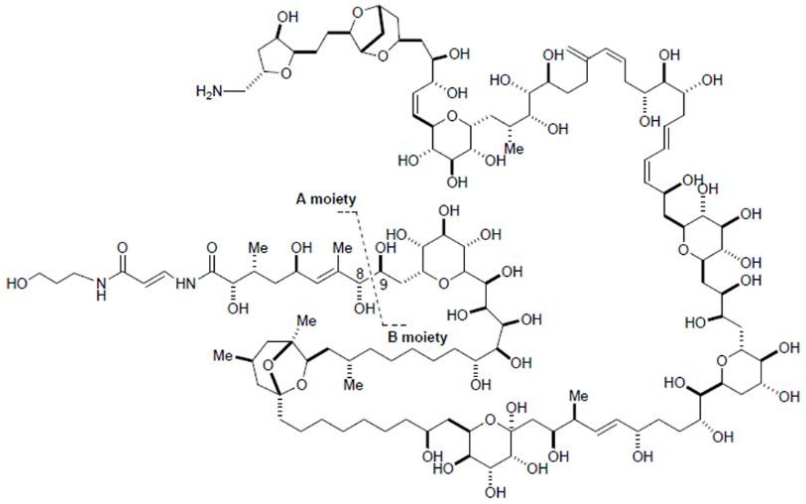

Toxin	M	A moiety	B moiety
Palytoxin	$C_{129}H_{223}N_3O_{54}$	$C_{16}H_{28}N_2O_6$	$C_{113}H_{195}NO_{48}$
Ovatoxin-a	$C_{129}H_{223}N_3O_{52}$	$C_{16}H_{28}N_2O_6$	$C_{113}H_{195}NO_{46}$
Ovatoxin-b	$C_{131}H_{227}N_3O_{53}$	$C_{18}H_{32}N_2O_7$	$C_{113}H_{195}NO_{46}$
Ovatoxin-c	$C_{131}H_{227}N_3O_{54}$	$C_{18}H_{32}N_2O_7$	$C_{113}H_{195}NO_{47}$
Ovatoxin-d	$C_{129}H_{223}N_3O_{53}$	$C_{16}H_{28}N_2O_6$	$C_{113}H_{195}NO_{47}$
Ovatoxin-e	$C_{129}H_{223}N_3O_{53}$	$C_{16}H_{28}N_2O_7$	$C_{113}H_{195}NO_{46}$

Figure 1. Structure of palytoxins. Molecular formulae (M) of ovatoxins and elemental composition of their relevant A and B moieties.

PlTX analogs have been detected in a wide range of marine animals, such as finfish, echinoderms, gastropods, crustaceans, and cephalopods, without any apparent sign of harm to these organisms [35,36]. *Ostreopsis* blooms have been often associated with anomalous arm positions in starfish and the loss of spines in sea urchins in Mediterranean waters (northern Tyrrhenian Sea) [37], as well as mass mortalities of sea urchins along Brazilian [38] and New Zealand coasts [39]. In laboratory experiments, *O.* cf. *ovata* was shown to be harmful to the larvae of jellyfish [40], invertebrates, and finfish [41,42]. Impairments observed consisted of sperm fertility reduction [43] and abnormal growth in embryos produced via the fertilization of sea urchins during blooms [44,45]. In mussels, high concentrations of PlTX analogs may cause an evident decrease in metabolic rates in hepatopancreas and mantle cells [46] or increase the percentage of phagocytizing immunocytes [47]. Mussel susceptibility to *Ostreopsis* was shown in the inhibition of the Na^+/K^+ ATPase and the alteration of other enzymatic activities [48], as well as in immunopathological signals [49]. Mussels exposed to *Ostreopsis* activated an inflammatory response, mainly characterized by digestive tubule damage and hemocyte aggregates, preventing further feeding and food assimilation [50].

In particular, in the Mediterranean Sea, PlTX analogs were detected in shellfish collected from the northern Aegean Sea, the French Mediterranean coasts, the northern Adriatic Sea, and the Gulf of Naples, with maximum concentrations ranging from 100 to 600 μg kg^{-1} [51–54]. These concentrations are much higher than the threshold of 30 μg kg^{-1} indicated by the European Food Safety Authority [55]. Therefore, although there is evidence of shellfish contamination by *Ostreopsis* toxins in temperate areas, the dynamics of their bioaccumulation during the entire period of an *Ostreopsis* bloom are not clear yet. Consequently, the potential health risks related to mussel consumption in the course of a bloom are also poorly understood.

The aim of this study was to investigate the accumulation of PlTX analogs in natural mussel banks during an *Ostreopsis* cf. *ovata* bloom that occurred in late summer/early fall

in 2021 in an area considered a hot-spot for the blooms of this toxic dinoflagellate (Conero Riviera, northern Adriatic Sea, Italy) [18]. The results of this study will help to better define the risks associated with the consumption of contaminated mussels during the occurrence of these phenomena.

2. Materials and Methods

2.1. Sampling

The study was carried out along the Conero Riviera (northern Adriatic Sea) at two stations, Passetto (43°37′09″ N, 13°31′54″ E) and Portonovo (43°33′41″ N 13°36′06″ E) (Figure 2). The shallow part of the sea bottom (1–5 m) at these stations is rocky and gently sloping, partially covered by cobbles and coarse gravel. The Passetto station is a sheltered site, whereas Portonovo is affected by moderate hydrodynamics. Both stations are affected by moderate human effects, as the shore is a popular area for summer holidays. There, mussels from natural banks are collected for human consumption by swimmers in summer and autumn.

Samples of wild mussels were collected at both stations. Samples for *Ostreopsis* analysis were collected only at the Passetto station.

Mussel (*Mytilus galloprovincialis*) samples were collected with approximately weekly frequency from natural banks from August to October 2021, i.e., during the *O.* cf. *ovata* bloom. In consideration of the bioaccumulation time of toxins, mussel sampling was carried out 4–6 days after each *Ostreopsis* sampling. About thirty mussels of commercial size (5–7 cm in length) were collected manually via scuba diving and were transported to the laboratory.

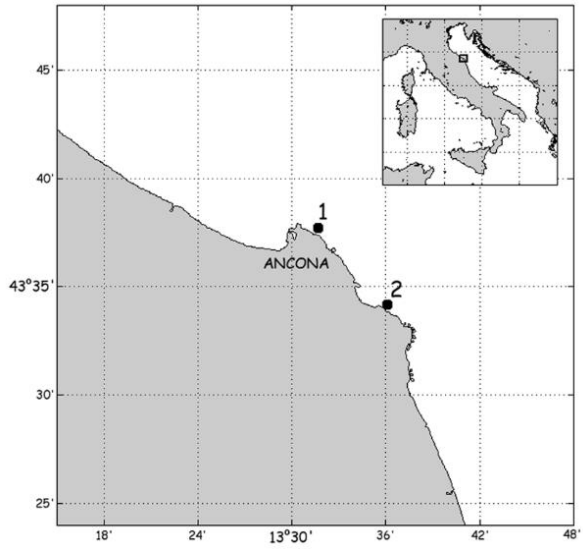

Figure 2. Map of the study area, showing the location of the sampling stations along the Conero Riviera (northern Adriatic Sea). 1: Passetto; 2: Portonovo.

Sampling of *Ostreopsis* cf. *ovata* was conducted monthly from May to July 2021 and weekly from August to October 2021 (i.e., when the bloom ended) at the Passetto station both on benthic substrata (macroalgae) and in the water column. A CTD, Model 30 Handheld Salinity, Conductivity and Temperature System, YSI (Yellow Spring, OH, USA), was used to measure sea surface temperature and salinity and wave height was recorded according to the Douglas scale. For nutrient analysis, water samples were collected near the sampled substratum, avoiding resuspension phenomena, in polyethylene bottles (50 mL); immediately filtered through GF/F Whatman filters (25 mm); and stored in triplicate in 4 mL polyethylene bottles at −22 °C until analysis. Fragments of macroalgal thalli, i.e., *Alsidium corallinum*, *Hypnea musciformis* (Florideophyceae, Rhodophyta), *Dictyota dichotoma*, and *Dictyopteris polypodioides* (Phaeophyceae, Ochrophyta) were collected in three replicates at a

depth of 0.5 m, following the protocol recommended by Totti et al. [56]. On each sampling date, samples of surface seawater (1 replicate) were collected in polyethylene bottles (500 mL) near the sampled macroalgae to analyze the abundance of *Ostreopsis* cf. *ovata* in the water column.

2.2. Mussel Sample Treatment

The mussel samples were prepared within 24 h of arrival in the laboratory to prevent the processes of metabolizing toxins. The valves were opened, cleaned, and any residual sand and solids were removed with running water. The mollusk flesh was separated from the shell by removing it with a metal scalpel and was then placed in a large mesh sieve to remove excess water. The pulp was then finely chopped with a blade homogenizer, obtaining a representative sample of 100 g from about 20 specimens used. The homogenate was transferred to a plastic jar and stored at −20 °C until analysis.

2.3. Ostreopsis Sample Treatment

In the laboratory, macroalgae were immediately treated following the method of Totti et al. [56]. Briefly, in the field, samples of macroalgae were vigorously shaken in wide-necked HDPE sample bottles in ~100 mL of seawater to dislodge the epiphytic cells. The samples were preserved with 0.8% neutralized formaldehyde [57] and stored in the dark at 4 °C until microscopic observation. Finally, the macroalgae were weighed to assess their fresh and dry weights, and their area was calculated using a conversion factor obtained from the ratio of fresh weight/surface, following the method of Accoroni et al. [54]. Some subsamples without the addition of any fixative were used for strain isolation (see below).

2.4. Microscopic Analysis of Ostreopsis

The estimation of *Ostreopsis* abundances was performed using an inverted microscope (Zeiss Axiovert 135) equipped with phase contrast, at 200× magnification. Sub-samples (1–25 mL) were settled in counting chambers after homogenization, according to the Utermöhl sedimentation method [58]. Cells of *O.* cf. *ovata* were identified by observing samples in epifluorescence after staining with a fluorochrome (Calcofluor White). Counting was performed on 10–30 random fields, 1–2 transects, or the whole sedimentation chamber, to count a representative cell number. The final data were expressed as cells g^{-1} fw/dw and cells cm^{-2} of macroalga, and as cells L^{-1} for the water column.

2.5. Strain Isolation, DNA Extraction, Amplification, and Sequencing

Ostreopsis cell isolation was conducted following the capillary pipette method [59]. After an initial growth period on microplates, cells were cultured with a 12:12 h L:D photoperiod and an irradiance of 90–100 µmol m^{-2} s^{-1} at 21 °C ± 0.1 °C in a modified, silica-free, f/4 medium [60] prepared with autoclaved natural seawater (salinity 35). Trace metals, vitamins (H, B1, and B12), and HEPES pH 7.1 were added at levels corresponding to the f/2 medium. Two strains of *Ostreopsis* sp. were isolated.

A 30 mL culture of each strain in the exponential growth phase was used to extract genomic DNA. The sample was centrifuged at 4000× *g* for 15 min and DNA was extracted using the CTAB (N-cetyl-N,N,N-trimethylammonium bromide) buffer (2% CTAB, 1 M Tris pH 8.0, 0.5 M EDTA pH 8.0, 5 M NaCl, 1%) modified from the method of Doyle and Doyle [61]. Extracted DNA was amplified by means of a polymerase chain reaction (PCR) with a SimpliAmp™ Thermal Cycler (Thermo Fisher Scientific, Waltham, MA, USA). PCR amplification of region D1–D3 of the LSU rDNA gene was performed following the method of Accoroni et al. [62].

Sanger sequencing was carried out by Macrogen Europe using the same couple of universal primers used for PCR amplification (D1R–D3Ca [63]). Sequences were compared to the NCBI database via a BLAST search with default settings (https://blast.ncbi.nlm.nih.gov/Blast.cgi, accessed on 17 December 2021), confirming the identification of *Ostreopsis* cf. *ovata* (showing > 99% of identity with *Ostreopsis* cf. *ovata* LSU sequences from GenBank).

2.6. Chemical Analysis of PlTX Analogs

2.6.1. Chemicals and Standards

Acetonitrile (MeACN, HPLC-MS grade) and methanol (MeOH, HPLC grade) were obtained from CARLO ERBA Reagents S.r.l. (Milano, Italy) and acetic acid (CH_3COOH, HPLC-MS grade) was acquired from (Steinheim, Germany). Water 18 mΩ pure (DIW) was produced by means of a Milli Q water purification system (Millipore Ltd., Bedford, MA, USA).

A non-certified analytical standard of PlTX (CAS RN: 77734-91-9, assay 85.8%) was obtained from Wako Chemicals GmbH (Neuss, Germany) as a colorless film (100 µg). Before use, it was dissolved in 5 mL of MeOH/H_2O (1:1, v/v), obtaining a stock solution of 20 µg mL^{-1}.

A matrix-matched standard of PlTX, at five levels of concentration (0.080, 0.125 0.250, 0.5, and 1.5 µg mL^{-1}), was prepared to build calibration curves for quantitative analyses. A mussel tissue reference material, certified as negative control (CRM-Zero_Mus), was purchased from the National Research Council Certified Reference Materials Program (Institute for Marine Biosciences, Halifax, NS, Canada) and used to prepare the calibration curves.

The PlTX standard was used to quantify PlTX analogs, assuming an equimolar response.

2.6.2. PlTX Analog Extraction from Mussels

The extraction of PlTX analogs from mussels was performed following the procedure described by Ciminiello et al. [64] with some modifications to improve sensitivity.

Briefly, 10.0 g ± 0.5 g of mussel homogenate was weighted in a 50 mL PP tube and added to 30 mL of MeOH/H_2O (80:20 v/v). The sample was then homogenized using an Ultra Turrax T25 mixer for 2 min at 9500 rpm and centrifuged for 15 min at 2000× g (20 °C). The supernatant was transferred in a 100 mL evaporation flask and the solid residue was re-extracted twice times in the same conditions described above. The supernatants were collected, obtaining a final volume of 90 mL and evaporated to dryness (T = 50–60 °C) via rotary evaporation (R-114 Büchi, Flawil, Switzerland).

The residue was reconstituted in 5 mL of MeOH/H_2O (80:20 v/v) and filtered through a 0.2 µm syringe filter for LC-MS/MS analysis.

2.6.3. LC-MS/MS Analysis

LC-MS/MS analyses were performed on a 3200 QTRAP mass spectrometer (AB Sciex, Darmstadt, Germany) equipped with an electrospray ionization (ESI) interface, coupled to a 1200 series HPLC system (Agilent, Palo Alto, CA, USA), including a solvent reservoir, inline degasser, quaternary pump, refrigerated autosampler, and column oven.

The method was performed following the conditions described previously [54,64], with slight modifications. LC separation was obtained by means of a Gemini NX-C18 column (2 mm × 100 mm, 3 µm particle size; Phenomenex, Torrance, CA, USA), thermostated at 40 °C, using a flowrate of 0.2 mL min^{-1} and an injection volume of 10 µL. Mobile phases A and B were H_2O and MeACN/H_2O (95:5 v/v), respectively, both containing 30 mM of CH_3COOH. Gradient elution was performed as follows: from 0% to 50% B in 20 min, from 50% to 100% B in 10 min, hold for 5 min, return to the original conditions at 40 min, and hold for 10 min before the next injection.

Infusion experiments with the PlTX standard were conducted to set the turbo IonSpray source parameters as follows: nebulizer gas (GS1) 40 psi, auxiliary gas (GS2) 20 psi, temperature (TEM) 600 °C, ion spray voltage (IS) 5000 V, curtain gas (CUR) 20 psi.

Multiple reaction monitoring (MRM) with positive spray ionization was performed by selecting the following transitions: PlTX/isobPlTX m/z 1340.7 → 327.1 and m/z 1331.7 → 327.1, OVTX-a m/z 1324.7 → 327.1 and m/z 1315.7 → 327.1, OVTX-b m/z 1346.3 → 371.2 and m/z 1337.3 → 371.2, OVTX-c m/z 1354.3 → 371.2 and m/z 1345.3 → 371.2, OVTX-d m/z 1332.3 → 327.1 and m/z 1323.3 → 327.1, OVTX-e m/z 1332.3 → 343.1, and m/z 1323.3 → 343.1. A collision energy (CE) of 40 eV and a dwell time of 100 ms were used for all transitions.

Relative retention times (RRTs) were also used to identify PlTX analogs using the PlTX standard. The method was validated in house in order to obtain good performances in terms

of linearity, recovery, matrix effect, repeatability (data not shown), the limit of quantification (LOQ), and the limit of detection (LOD). The LOQ, calculated assuming a signal/noise (S/N) ratio of 10, was 13 μg kg^{-1}, whereas the LOD (S/N ratio of 3) was 5 μg kg^{-1}.

2.6.4. UHPLC-HRMS^2 Analysis

UHPLC-HRMS^2 analysis was performed using a hybrid quadrupole-Orbitra Q-Exactive mass spectrometer, working in tandem mass spectrometry mode (Thermo Fisher). The mass spectrometer was coupled to a UHPLC system (Thermo Fisher) equipped with a solvent reservoir, a quaternary pump, a refrigerated autosampler, and a column oven.

LC separation was performed using a Luna PFP 2 column (2 mm × 150 mm, 3 μm particle size from Phenomenex) at 40 °C, at a 0.2 mL min^{-1} flow rate and a 10 μL injection volume. The mobile phases were (A) Water and (B) Acetonitrile/Water 95/5 in volume, both containing 0.1% (*v*/*v*) of CH_3COOH. The elution was performed with a linear gradient: from 20% to 70% B in 25 min, from 70% to 98% B in 0.5 min, hold for 5 min, then down to 20% B at 35 min.

HRMS^2 analysis was performed in negative ion mode (ESI-), setting the ion spray source parameters as follows: sheath gas flow rate—50 psi, auxiliary gas flow rate—15 psi, auxiliary gas heater temperature—325 °C, ion spray voltage—3.20 kV, resolution—70,000, and capillary temperature—275 °C.

For each toxin, the molecular precursor ion and 1 or 2 product ions were monitored, with a mass accuracy greater than 5 ppm, as indicated in Table 1.

Table 1. Precursor and product ions of palytoxin analogs.

Toxin	Precursor Ion (*m*/*z*)	Product Ions (*m*/*z*)
PlTX	1338.735884	1450.758–1151.669–903.531
OVTX-a	1322.740970	1434.763–1135.674–887.537
OVTX-b	1344.754077	1434.763–1179.700–887.537
OVTX-c	1352.751534	1434.763–1195.695–887.537
OVTX-d	1330.738427	1450.758–1135.674–887.537
OVTX-e	1330.738427	1434.763–1151.669–887.537

The method was based on the quantification of palytoxins by means of a calibration line with a matrix standard, in a measuring range ≥ 1 μg kg^{-1} of the sample as is (LOQ). By analyzing the trend of the product ions detected in the MS/MS spectrum characteristic of molecules similar to palytoxin, it was possible to identify and quantify them.

2.7. Nutrient Analysis

The colorimetric method of Strickland and Parsons [65] was used to perform the analysis of nitrates, nitrites, ammonium, phosphates and silicates, using an Autoanalyzer QuAAtro Axflow. Detectability limits were 0.02 μmol L^{-1} for nitrates, nitrites, ammonia, and silica and 0.03 μmol L^{-1} for orthophosphates. The dissolved inorganic nitrogen (DIN) concentration represents the sum of NO_2^-, NO_3^-, and NH_4^+ concentrations

2.8. Statistical Analysis

Comparisons between Spearman's (r_s) and Pearson's (r) correlations were undertaken to determine both monotonic and linear relationships between (i) the abundances of *Ostreopsis* cf. *ovata* recorded in the water column and on benthic substrate and (ii) the abundances of *Ostreopsis* cf. *ovata* and OVTX concentrations recorded in the soft tissue of mussels at Passetto station. The statistical analyses were conducted using Statistica (StatSoft) software.

3. Results

3.1. Ostreopsis Bloom

The first cells of *Ostreopsis* cf. *ovata* on the benthic substrata were recorded on 19 August and the bloom developed reaching the maximum abundances approximately one

month later, i.e., on 16 September ($4.9 \times 10^3 \pm 2.3 \times 10^3$ cells cm^{-2}, corresponding to $1.2 \times 10^5 \pm 5.9 \times 10^4$ cells g^{-1} fw and $9.9 \times 10^5 \pm 4.6 \times 10^5$ cells g^{-1} dw). During this period of maximum proliferation, the characteristic brownish mucilaginous biofilm produced by *Ostreopsis* covered all the macroalgae and the other benthic substrata. Then, around mid-September the abundances rapidly decreased to values around 10^3 cells cm^{-2}, although the bloom ended only in late October (Figure 3).

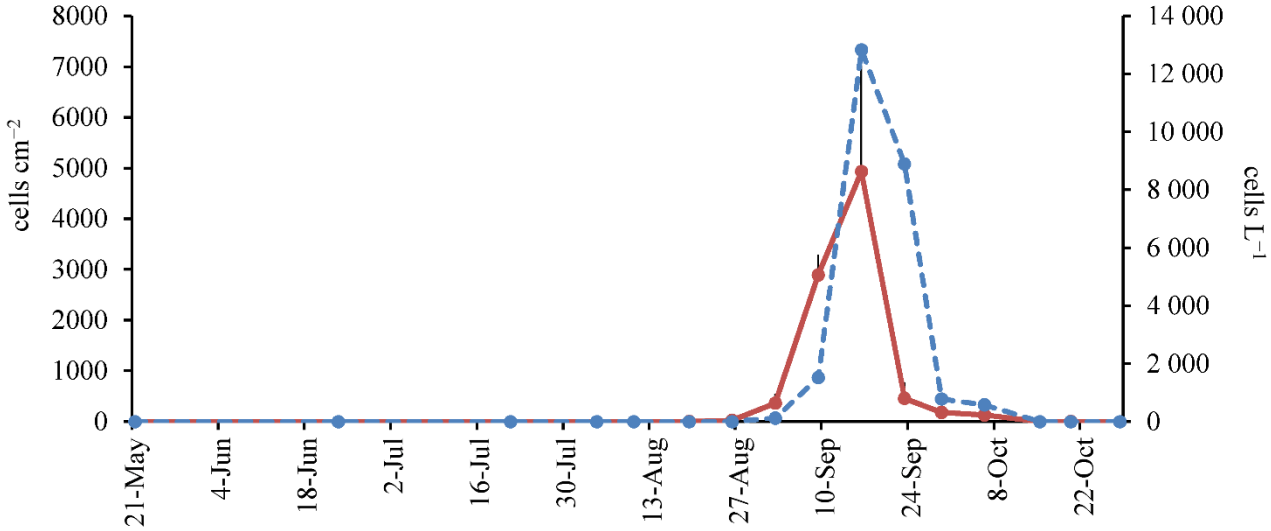

Figure 3. Abundance pattern of *Ostreopsis* cf. *ovata* on seaweeds (bold line, cells cm^{-2}, left y-axis) and in the water column (dotted line, cells L^{-1}, right y-axis) at the Passetto station. Error bars indicate standard deviation.

The abundance pattern of *Ostreopsis* cf. *ovata* in the water column closely followed that of the *Ostreopsis* abundances on macroalgae; the first cells in the water column were recorded on 2 September and the highest abundances were recorded on 16 September (as for the macroalgae) with 1.3×10^4 cells L^{-1}. Then, abundances decreased until early October and *O.* cf. *ovata* cells were no longer recorded in the water column by mid-October (Figure 3). The correlation between the abundance of *O.* cf. *ovata* on macroalgae and its abundance in the water column was positive and significant ($n = 16$; $r = 0.7595$; $r_s = 0.8944$; $p < 0.001$).

3.2. Environmental Parameters and Their Relationships with Blooms

During the bloom period, the sea surface temperature ranged from 26.5 °C to 16.4 °C, and salinity from 36.4 to 30.7. At the start of the bloom, the water temperature reached the highest values (26.5 °C), whereas at the bloom peak (mid-September 2021) the temperature was 24.2 °C. Then, when the temperature decreased to values below 20 °C, the bloom rapidly declined (Figure 4). Concentrations of DIN ranged from 0.978 to 13.324 µmol L^{-1} (2 September and 15 October, respectively). NH_4^+ and NO_3^- were the main contributors to DIN (Figure 5). The concentrations of PO_4^{3-} ranged from 0.03 to 0.467 µmol L^{-1}. The three highest PO_4^{3-} values were detected around the start of the bloom (0.162 µmol L^{-1}), at the bloom peak (0.151 µmol L^{-1}), and near the end of the bloom (0.467 µmol L^{-1}), whereas PO_4^{3-} values generally did not exceed 0.100 µmol L^{-1} during the rest of the bloom (Figure 5).

The ratios of inorganic N:P ranged from 19 to 164 during the bloom. Values above 50 were recorded by the end of September, when the *O.* cf. *ovata* bloom was approaching its end. N:P values close to 16 (i.e., the Redfield ratio) were recorded just before the bloom's onset (13–14) and during the bloom's peak (19) (Figure 4). The bloom dynamics were affected by hydrodynamism. Sea conditions were calm until the end of August, (i.e., at the time of the bloom's onset) and during the bloom's peak (Figure 4), whereas in mid-September the sea conditions became rougher (Douglas scale ≥ 2). At this time,

a sharp decrease in abundance was recorded on the substrata, not always followed by a proportional decrease in the water column (e.g., on 23 September). The bloom declined rapidly by the end of September, in correspondence with moderate–high hydrodynamic conditions (Douglas scale ≥ 2, i.e., wave height from 0.1 to 2.5 m, from smooth to moderate), although sporadic cells were recorded until the second part of October.

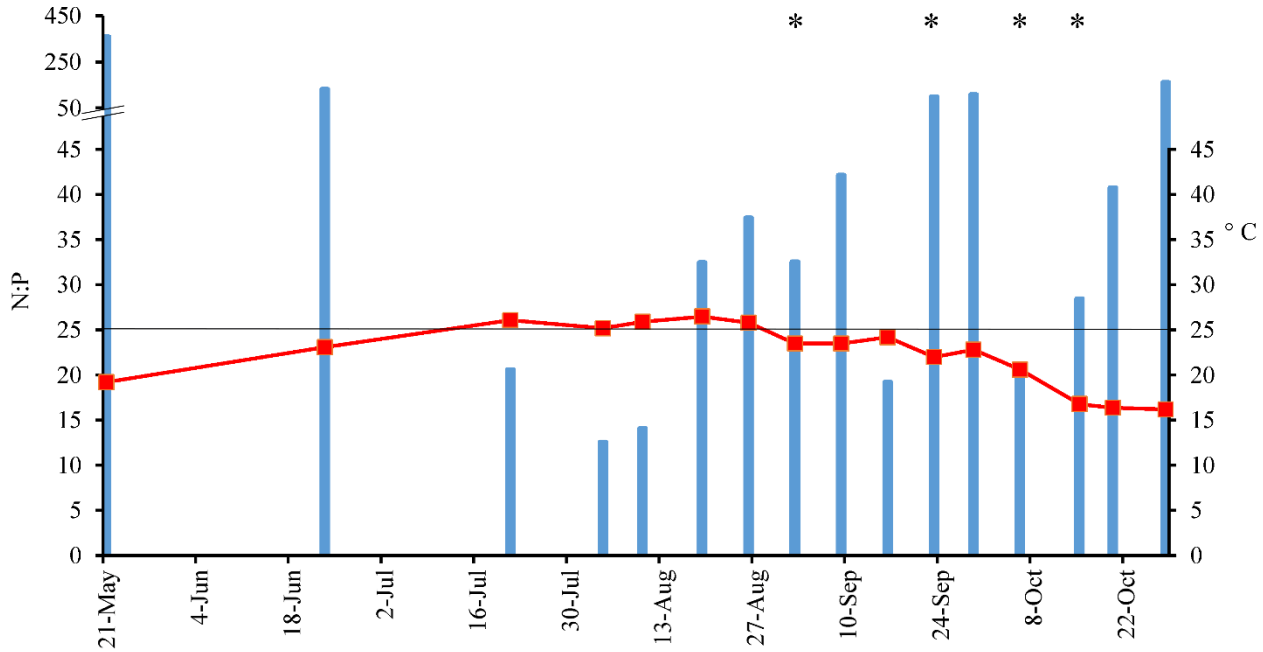

Figure 4. Temporal variability of the N:P ratio (bars, left y-axis) and water temperature (line, °C, right y-axis) at the Passetto station. The horizontal line represents both (i) the upper N:P ratio threshold, below which better nutrient conditions are supplied to *Ostreopsis* cf. *ovata* growth, and (ii) the lower temperature threshold, permitting the bloom's onset [66]. * denotes dates when sea conditions could potentially disturb the development of the bloom (Douglas scale ≥ 2, i.e., wave heights from 0.1 to 2.5 m, ranging from smooth to moderate).

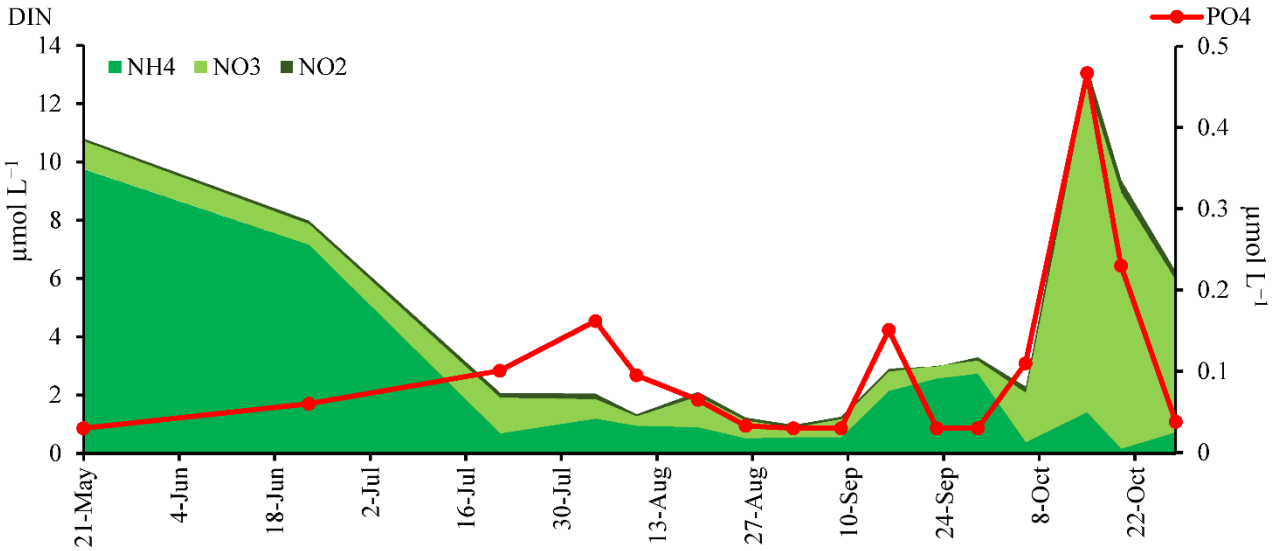

Figure 5. Trends of inorganic nutrient concentrations (µmol L^{-1}) at Passetto station: DIN with the details of the NO_3^-, NO_2^-, and NH_4^+ contributions (left y-axis) and that of PO_4^{3-} (line, right y-axis).

3.3. Temporal Trend of OVTXs Detected in Mussels and its Relationship with Ostreopsis cf. ovata Blooms

OVTX was the most abundant toxin (71%–74%) among the PlTX analogs detected in mussels, followed by OVTX-b (26%–29%) (Figure 6). At Passetto, OVTX was first recorded in the mussels sampled on 20 September (i.e., 32 days after the appearance of *O.* cf. *ovata* on macroalgae and 18 days after the first record in the water column) with a concentration of 15.8 and 15.7 µg kg^{-1} of soft tissue (LC-MS/MS and UHPLC-$HRMS^2$ results, respectively). These represented the highest values of OVTXs detected in this station (Figure 7). This peak of bioaccumulation in mussels was recorded 4 days after the recording of the bloom peak on 16 September. At the subsequent sampling date (27 September), OVTX concentrations were drastically lower, i.e., <LOD (5.0 µg/kg and 1.0 µg/kg for LC-MS/MS and UHPLC-$HRMS^2$, respectively). The same pattern was observed for the abundances of *Ostreopsis* (4 days before, abundances of *O.* cf. *ovata* were 456 cells cm^{-2} and 8.9 x 10^3 cells L^{-1} on macroalgae and in the water column, respectively). After 14 consecutive days without records of *O.* cf. *ovata* in seawater, OVTXs were no longer detected in mussels. A significant positive Pearson's correlation was found between *O.* cf. *ovata* abundances on macroalgae and OVTXs in mussels (n = 7; r= 0.8336; $p < 0.05$). A similarly positive correlation was found between *O.* cf. *ovata* abundances in the water column and OVTXs recorded in mussels (n = 7; r= 0.8574; $p < 0.05$).

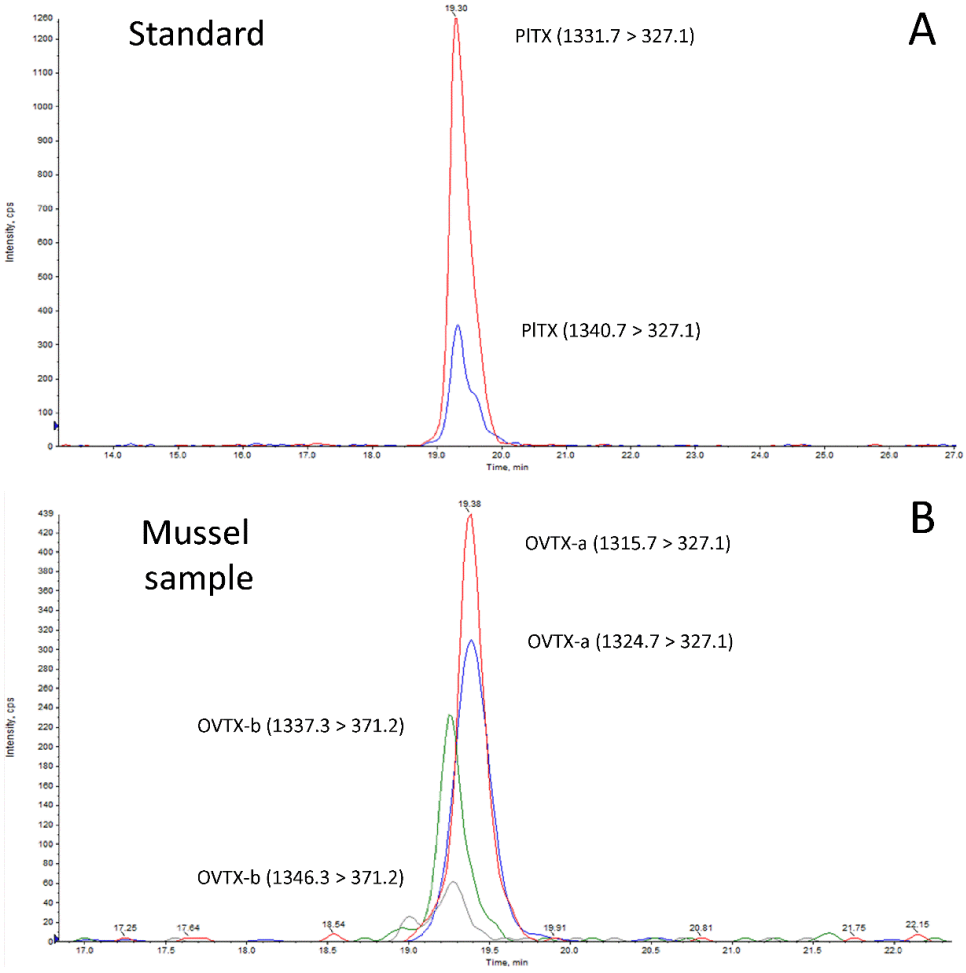

Figure 6. LC-MS/MS chromatograms of the (**A**) PlTX matrix-matched standard, (**B**) OVTX-a, and OVTX-b in the sample from Portonovo from 20 September. 1331.7 > 327.1, 1315.7 > 327.1, 1337.3 > 371.2 multiple reaction monitoring (MRM) transitions for PlTX, OVTX-a, and OVTX-b quantification, respectively. 1340.7 > 327.1, 1324.7 > 327.1, 1346.3 > 371.2, MRM transition for PlTX, OVTX-a, and OVTX-b confirmation, respectively.

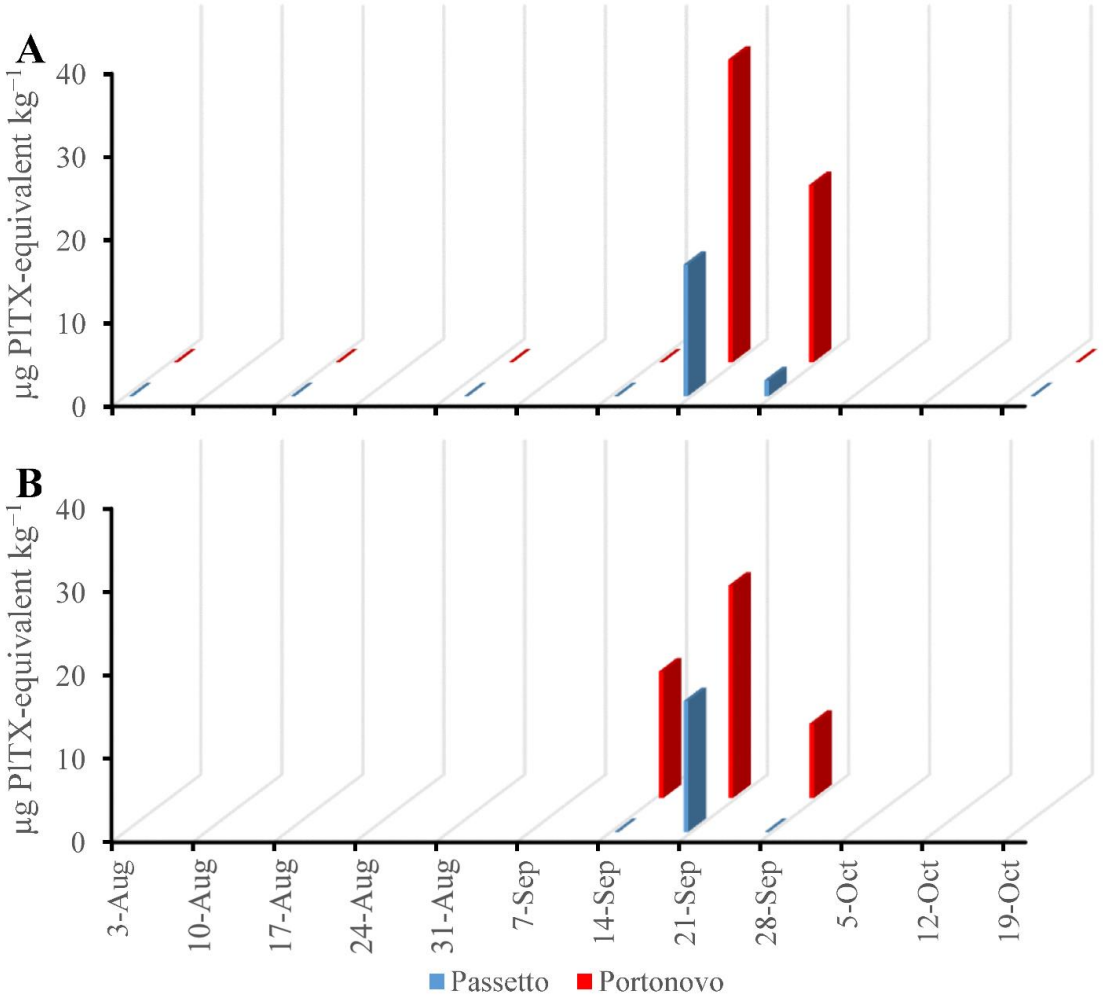

Figure 7. LC-MS/MS (**A**) and (**B**) UHPLC-HRMS^2 results showing the trends in the total content of palytoxin analogs (µg PlTX-equivalent kg^{-1} of soft tissue) in mussels collected from natural banks at sampling stations (light-blue) Passetto and (red) Portonovo.

Moreover, comparisons between Pearson's and Spearman's correlations of *O.* cf. *ovata* abundances in the water column and OVTXs recorded in mussels showed a monotonic rather than linear relationship (n = 7; r_s= 0.8846; $p < 0.01$). Conversely, no significant Spearman's correlation was observed between *O.* cf. *ovata* abundances on macroalgae and OVTXs recorded in mussels (n = 7; 0.6742; $p > 0.05$).

At Portonovo, OVTXs were first recorded in mussels on 20 September using the LC-MS/MS method and on 14 September using the UHPLC-HRMS^2 method. Maximum concentrations were recorded in mussels collected on 20 September (36.4 and 25.5 µg kg^{-1} of soft tissue, LC-MS/MS, and UHPLC-HRMS^2 results, respectively).

4. Discussion

Although blooms of *Ostreopsis* cf. *ovata* have been constantly reported along the Conero Riviera in the late summer/early autumn period since 2006 [54,56,67], the bioaccumulation of PlTX analogs produced during this phenomenon in edible invertebrates has been poorly studied. The European Legislation, with Regulation No. 853/2004 and subsequent amendments, limits the commercialization of bivalve mollusks for human consumption when contaminated by phycotoxins, setting a maximum level for each toxin except for some compounds called 'emerging marine biotoxins', e.g., tetrodotoxins, cyclic imines, and palytoxins, for which an EU regulation has not yet been established. In 2006, the European Food Safety Authority (EFSA) received a request from the European Commis-

sion (EC) to develop a series of scientific opinions concerning these marine biotoxins. The EFSA indicated 30 μg kg^{-1} as threshold value for PlTX, above which PlTX-contaminated mollusks would be unsafe for consumers [55].

In this study, we showed that, in the Conero Riviera, wild mussels bioaccumulated PlTX-equivalent concentration at levels generally lower than the EFSA threshold. The only exception was recorded for Portonovo on 20 September 2021, with 36.4 μg kg^{-1} of soft tissue (LC-MS/MS). This finding highlights the necessity of characterizing the hazard posed by oral exposure to these toxins, which still represents a major gap in our knowledge [31]. The observed toxin profile fits well with the profile previously detected in field samples of *O*. cf. *ovata* populations in the same study area [68]. This is the most common toxin profile of *O.* cf. *ovata* strains from the Mediterranean area [69], dominated by OVTX-a, followed by OVTX-b, -d, -e, -c, and isobPlTX, in decreasing order of percentage. However, in our samples the contributions of OVTX, -d, -e, -c, and isobPlTX were undetectable, probably because such toxins represented a very minor component of the profile, as suggested by Accoroni et al. [67].

The finding that contaminated mussels showed the same toxin profile as that of the toxigenic microalga blooming in the area was not so obvious. It is well known that phycotoxins can be subjected to biotransformation, and/or to a differential accumulation/excretion equilibrium related to the molecular properties of each compound after their ingestion by invertebrates. Such processes have been described for paralytic shellfish toxins (PSTs [70]), diarrhoetic shellfish toxins [71], and azaspiracids [72,73].

The results of this study support the concept that the bioaccumulation of toxins in wild mussels does not depend only on the abundances of toxic microalgae. Indeed, although higher abundances of *Ostreopsis* have been recorded in Passetto than in Portonovo since 2006 (https://www.arpa.marche.it/balneazione-nuovo/ostreopsis-cf-ovata, accessed on 18 April 2022), mussels bioaccumulated higher OVTX concentrations at the latter site, exceeding the EFSA threshold. Several biotic and abiotic factors (intrinsic or non-intrinsic to the vector organisms) play a certain role in this process. First, algal growth and toxin production (and, therefore, algal abundances and toxin content) are not necessarily correlated, as they are influenced by different environmental parameters and by the physiological status/life cycle stage of the alga [68,74,75]. Moreover, these two sites have different characteristics, which, regardless of the abundance of *Ostreopsis*, might affect the assimilation/detoxification rate in mussels. Bioaccumulation depends on several boundary conditions, such as the abundance and quality of the whole phytoplankton communities that affect the filtration rates [76], the nature of the contaminating toxins, and the physiology of the shellfish [77] and its history of exposure to toxins [78]. Indeed, the modulation of filtration (and/or rejection) capacity is a behavioral response that is common in bivalves exposed to toxic microalgae (e.g., PST-producing species [79]). In particular, in laboratory experiments carried out on mussels fed on *O.* cf. *ovata*, Sardo et al. [51] observed that the ratio between mussel size and cell concentration, rather than the simple cell densities, affected the filtration rates of the invertebrates. Moreover, Gorbi et al. [49] observed inhibition of the feeding activity in mussels exposed to *Ostreopsis* cf. *ovata*. Therefore, as mussels from Passetto are generally exposed to higher *Ostreopsis* abundances than those from Portonovo [54,56], paradoxically they could accumulate fewer toxins, being inhibited in their filtration rate.

Previous papers have extensively discussed the role of hydrodynamics, temperature, nutrients, and depth on the dynamics of *Ostreopsis* cf. *ovata* blooms in the Conero Riviera. This area is a shallow coast, which is strongly phosphorus limited [80]. Calm sea conditions, temperatures > 25 °C, and the increased availability of inorganic phosphorus leading to N:P ratios reaching the Redfield ratio are known to be ideal conditions for the onset of *Ostreopsis* blooms. These conditions also favor the blooms' development, as long as sea surface temperatures remain >20 °C [66]. The results of this study confirm once again this bloom mechanism: bloom onset occurred at 26.5 °C (i.e., the yearly maximum), after days with low

hydrodynamism, and a high level of inorganic P and an N:P ratio close to the Redfield ratio. High levels of P and optimal N:P values were also recorded during the bloom peak.

A clear and crucial role of the hydrodynamic conditions in the development of *Ostreopsis* blooms has been previously recognized. Blooms occur even in exposed sites, but higher abundances are detected under sheltered conditions [39,56,81–83]. Higher abundances have been historically observed in Passetto, the sheltered station, than in the more exposed Portonovo station [54,56] (https://www.arpa.marche.it/balneazione-nuovo/ostreopsis-cf-ovata, accessed on 18 April 2022). Moreover, intense hydrodynamic events may influence the correlation between the abundances of *O.* cf. *ovata* in the water column and on benthic substrata. The *O.* cf. *ovata* biofilm is merely attached to the substrate and is easily resuspended in the water column. Therefore, strong hydrodynamism can either increase abundances in the water column via resuspension (as happened in this study on 23 September) or, if a hydrodynamic event is very intense, it can decrease them via dilution (as happens each year at the end of the bloom). This also explains why correlations of benthic and planktonic abundances showed a monotonic rather than linear relationship. Given that *Ostreopsis* cells exhibit predominantly benthic behaviour, they can be transferred to the water column only under certain hydrodynamic conditions [5].

In this study, it was possible to recognize a clear correlation between the abundances of *O.* cf. *ovata* and the bioaccumulation of OVTXs' in mussels. The fact that this toxic species is benthic rather than planktonic may make it relatively unavailable as a food resource for filter-feeding shellfish except during periods when cells are resuspended in the water column and/or when the biofilm of benthic cells extends onto the mollusc shells. Indeed, although this correlation is observable with abundances of *O.* cf. *ovata* both on benthic substrates and in the water column, it is more evident with the latter, where the monotonic relationship suggests that other factors in addition to the abundances of *Ostreopsis* cells in water influence the bioaccumulation of toxins in filter-feeding shellfish.

In Italy, *Ostreopsis* blooms are managed following specific guidelines to protect human health in bathing waters affected by this phenomenon. These guidelines consider three phases based on *Ostreopsis* abundances in the water column [84]: routine ($\leq$10,000 cells L^{-1}), alert (10,000–30,000 cells L^{-1}), and emergency (>30,000 cells L^{-1}) phases. Looking at the monitoring data of *Ostreopsis* cf. *ovata* bloom collected by the Regional Environmental Protection Agency of Marche (ARPAM) at the Passetto and Portonovo stations in the summer/fall of 2021, a similar pattern was observed in both stations and in agreement with the values obtained in this study (Table S1). At both stations, mussels accumulated an appreciable amount of OVTXs only when the abundance of *Ostreopsis* in the water column reached the alert phase. Conversely, when its abundance in the water column declined to the routine phase, a few days later the mussels showed much lower bioaccumulation of OVTXs. This indicates that the Italian guidelines to protect human health in bathing waters affected by *O.* cf. *ovata* blooms are also useful in managing the risk of human intoxication through the ingestion of contaminated mussels.

Supplementary Materials: The following supporting information can be downloaded at: https://www.mdpi.com/article/10.3390/jmse10101402/s1, Table S1: Monitoring data of *Ostreopsis* cf. *ovata* abundances in the water column collected by ARPAM at the Passetto and Portonovo stations in summer/fall 2021. Data are highlighted following the Italian guidelines to protect human health in bathing waters affected by *O.* cf. *ovata* blooms [84]: green = routine phase ($\leq$10,000 cells L^{-1}); yellow = alert phase (10,000–30,000 cells L^{-1}); red = emergency phase (>30,000 cells L^{-1}).

Author Contributions: Conceptualization, S.A. and C.T.; methodology, S.B., M.S. and M.G.B.; formal analysis, S.A. and S.B.; investigation, M.U., F.N., S.B. and A.C.; resources, S.A.; data curation, S.A.; writing—original draft preparation, S.A.; writing—review and editing, S.A. and C.T.; visualization, S.A.; supervision, C.T.; project administration, S.A.; funding acquisition, S.A. and M.S. All authors have read and agreed to the published version of the manuscript.

Funding: This study was funded by the Italian Ministry of Health (Ricerca Finalizzata 2016), grant number GR-2016-02363211.

Institutional Review Board Statement: Not applicable.

Informed Consent Statement: Not applicable.

Data Availability Statement: All the data involved in this study are reflected in the relevant figures and tables, and there are no additional data to be provided.

Acknowledgments: The authors kindly acknowledge Luigi Barbetti for his support in *Ostreopsis* sampling and Fabio Rindi for the useful suggestions and assistance with identification of macroalgae.

Conflicts of Interest: The authors declare no conflict of interest.

References

1. Accoroni, S.; Totti, C. The toxic benthic dinoflagellates of the genus *Ostreopsis* in temperate areas: A review. *Adv. Oceanogr. Limnol.* **2016**, *7*, 1–15. [CrossRef]
2. Pavaux, A.-S.; Velasquez-Carjaval, D.; Drouet, K.; Lebrun, A.; Hiroux, A.; Marro, S.; Christians, E.; Castagnetti, S.; Lemée, R. Daily variations of *Ostreopsis* cf. *ovata* abundances in NW Mediterranean Sea. *Harmful Algae* **2021**, *110*, 102144. [CrossRef] [PubMed]
3. Parsons, M.L.; Aligizaki, K.; Bottein, M.-Y.D.; Fraga, S.; Morton, S.L.; Penna, A.; Rhodes, L. *Gambierdiscus* and *Ostreopsis*: Reassessment of the state of knowledge of their taxonomy, geography, ecophysiology, and toxicology. *Harmful Algae* **2012**, *14*, 107–129. [CrossRef]
4. Rhodes, L. World-wide occurrence of the toxic dinoflagellate genus *Ostreopsis* Schmidt. *Toxicon* **2011**, *57*, 400–407. [CrossRef] [PubMed]
5. Accoroni, S.; Totti, C.; Romagnoli, T.; Giulietti, S.; Glibert, P.M. Distribution and potential toxicity of benthic harmful dinoflagellates in waters of Florida Bay and the Florida Keys. *Mar. Environ. Res.* **2020**, *155*, 104891. [CrossRef]
6. Ballantine, D.L.; Tosteson, T.R.; Bardales, A.T. Population dynamics and toxicity of natural populations of benthic dinoflagellates in southwestern Puerto Rico. *J. Exp. Mar. Biol. Ecol.* **1988**, *119*, 201–212. [CrossRef]
7. Boisnoir, A.; Pascal, P.-Y.; Cordonnier, S.; Lemée, R. Depth distribution of benthic dinoflagellates in the Caribbean Sea. *J. Sea Res.* **2018**, *135*, 74–83. [CrossRef]
8. Boisnoir, A.; Pascal, P.-Y.; Cordonnier, S.; Lemée, R. Spatio-temporal dynamics and biotic substrate preferences of benthic dinoflagellates in the Lesser Antilles, Caribbean Sea. *Harmful Algae* **2019**, *81*, 18–29. [CrossRef]
9. Bomber, J.W.; Morton, S.L.; Babinchak, J.A.; Norris, D.R.; Morton, J.G. Epiphytic dinoflagellates of drift algae—Another toxigenic community in the ciguatera food chain. *Bull. Mar. Sci.* **1988**, *43*, 204–214.
10. Delgado, G.; Lechuga-Devéze, C.H.; Popowski, G.; Troccoli, L.; Salinas, C.A. Epiphytic dinoflagellates associated with ciguatera in the northwestern coast of Cuba. *Rev. Biol. Trop.* **2006**, *54*, 299–310. [CrossRef]
11. Díaz-Asencio, L.; Vandersea, M.; Chomérat, N.; Fraga, S.; Clausing, R.J.; Litaker, R.W.; Chamero-Lago, D.; Gómez-Batista, M.; Moreira-González, A.; Tester, P.; et al. Morphology, Toxicity and molecular characterization of *Gambierdiscus* spp. towards risk assessment of ciguatera in south central Cuba. *Harmful Algae* **2019**, *86*, 119–127. [CrossRef] [PubMed]
12. Faust, M.A. Ciguatera-causing dinoflagellates in a coral-reef mangrove ecosystem, Belize. *Atoll Res. Bull.* **2009**, *569*, 1–32. [CrossRef]
13. Okolodkov, Y.B.; Campos-Bautista, G.; Gárate-Lizárraga, I.; González-González, J.A.G.; Hoppenrath, M.; Arenas, V. Seasonal Changes of benthic and epiphytic dinoflagellates in the Veracruz Reef zone, Gulf of Mexico. *Aquat. Microb. Ecol.* **2007**, *47*, 223–237. [CrossRef]
14. Parsons, M.L.; Preskitt, L.B. A Survey of epiphytic dinoflagellates from the coastal waters of the island of Hawai'i. *Harmful Algae* **2007**, *6*, 658–669. [CrossRef]
15. Tester, P.A.; Kibler, S.R.; Holland, W.C.; Usup, G.; Vandersea, M.W.; Leaw, C.P.; Teen, L.P.; Larsen, J.; Mohammad-Noor, N.; Faust, M.A.; et al. Sampling harmful benthic dinoflagellates: Comparison of artificial and natural substrate methods. *Harmful Algae* **2014**, *39*, 8–25. [CrossRef]
16. Zenetos, A.; Cinar, M.E.; Pancucci-Papadopoulou, M.A.; Harmelin, J.G.; Furnari, G.; Andaloro, F.; Bellou, N.; Streftaris, N.; Zibrowius, H. Annotated list of marine alien species in the mediterranean with records of the worst invasive species. *Mediterr. Mar. Sci.* **2005**, *6*, 63–118. [CrossRef]
17. Corriero, G.; Pierri, C.; Accoroni, S.; Alabiso, G.; Bavestrello, G.; Barbone, E.; Bastianini, M.; Bazzoni, A.M.; Bernardi Aubry, F.; Boero, F.; et al. Ecosystem vulnerability to alien and invasive species: A case study on marine habitats along the Italian coast. *Aquat. Conserv. Mar. Freshw. Ecosyst.* **2016**, *26*, 392–409. [CrossRef]
18. Mangialajo, L.; Ganzin, N.; Accoroni, S.; Asnaghi, V.; Blanfuné, A.; Cabrini, M.; Cattaneo-Vietti, R.; Chavanon, F.; Chiantore, M.; Cohu, S.; et al. Trends in *Ostreopsis* proliferation along the Northern Mediterranean Coasts. *Toxicon* **2011**, *57*, 408–420. [CrossRef]
19. Vassalli, M.; Penna, A.; Sbrana, F.; Casabianca, S.; Gjeci, N.; Capellacci, S.; Asnaghi, V.; Ottaviani, E.; Giussani, V.; Pugliese, L.; et al. Intercalibration of counting methods for *Ostreopsis* spp. blooms in the Mediterranean Sea. *Ecol. Indic.* **2018**, *85*, 1092–1100. [CrossRef]
20. Brissard, C.; Hervé, F.; Sibat, M.; Séchet, V.; Hess, P.; Amzil, Z.; Herrenknecht, C. Characterization of ovatoxin-h, a new ovatoxin analog, and evaluation of chromatographic columns for ovatoxin analysis and purification. *J. Chromatogr. A* **2015**, *1388*, 87–101. [CrossRef]

21. Accoroni, S.; Romagnoli, T.; Penna, A.; Capellacci, S.; Ciminiello, P.; Dell'Aversano, C.; Tartaglione, L.; Abboud-Abi Saab, M.; Giussani, V.; Asnaghi, V.; et al. *Ostreopsis fattorussoi* sp. nov. (Dinophyceae), a new benthic toxic *Ostreopsis* species from the eastern Mediterranean Sea. *J. Phycol.* **2016**, *52*, 1064–1084. [CrossRef] [PubMed]
22. Nakajima, I.; Oshima, Y.; Yasumoto, T. Toxicity of benthic dinoflagellates in Okinawa. *Nippon Suisan Gakkaishi* **1981**, *47*, 1029–1033. [CrossRef]
23. Yasumoto, T.; Seino, N.; Murakami, Y.; Murata, M. Toxins produced by benthic dinoflagellates. *Biol. Bull.* **2007**, *172*, 128–131. [CrossRef]
24. Holmes, M.J.; Gillespie, N.C.; Lewis, R.J. Toxicity and morphology of *Ostreopsis* cf. *siamensis* cultured from a ciguatera endemic region of queensland, australia. In Proceedings of the 6th International Coral Reef Symposium, Townsville, Australia, 8–12 August 1988; Choat, J.H., Barnes, D., Borowitzka, M.A., Coll, J.C., Davies, P.J., Flood, P., Hatcher, B.G., Hopley, D., Hutchings, P.A., Kinsey, D., Eds.; Contributed Papers: Townsville, Australia, 1988; pp. 49–54.
25. Meunier, F.A.; Mercado, J.A.; Molgó, J.; Tosteson, T.R.; Escalona de Motta, G. Selective depolarization of the muscle membrane in frog nerve-muscle preparations by a chromatographically purified extract of the dinoflagellate *Ostreopsis lenticularis*. *Br. J. Pharmacol.* **1997**, *121*, 1224–1230. [CrossRef] [PubMed]
26. Lenoir, S.; Ten-Hage, L.; Turquet, J.; Quod, J.-P.; Bernard, C.; Hennion, M.-C. First evidence of palytoxin analogues from an *Ostreopsis mascarenensis* (Dinophyceae) benthic bloom in southwestern Indian Ocean. *J. Phycol.* **2004**, *40*, 1042–1051. [CrossRef]
27. Ciminiello, P.; Dell'Aversano, C.; Fattorusso, E.; Forino, M.; Magno, G.S.; Tartaglione, L.; Grillo, C.; Melchiorre, N. The Genoa 2005 outbreak. Determination of putative palytoxin in Mediterranean *Ostreopsis ovata* by a new liquid chromatography tandem mass spectrometry method. *Anal. Chem.* **2006**, *78*, 6153–6159. [CrossRef] [PubMed]
28. Uchida, H.; Taira, Y.; Yasumoto, T. Structural Elucidation of palytoxin analogs produced by the dinoflagellate *Ostreopsis ovata* IK2 strain by complementary use of positive and negative ion liquid chromatography/quadrupole time-of-flight mass spectrometry. *Rapid Commun. Mass Spectrom.* **2013**, *27*, 1999–2008. [CrossRef] [PubMed]
29. Onuma, Y.; Satake, M.; Ukena, T.; Roux, J.; Chanteau, S.; Rasolofonirina, N.; Ratsimaloto, M.; Naoki, H.; Yasumoto, T. Identification of putative palytoxin as the cause of clupeotoxism. *Toxicon* **1999**, *37*, 55–65. [CrossRef]
30. Randall, J.E. Review of clupeotoxism, an often fatal illness from the consumption of clupeoid fishes. *Pac. Sci.* **2005**, *59*, 73–77. [CrossRef]
31. Tubaro, A.; Durando, P.; Del Favero, G.; Ansaldi, F.; Icardi, G.; Deeds, J.R.; Sosa, S. Case definitions for human poisonings postulated to palytoxins exposure. *Toxicon* **2011**, *57*, 478–495. [CrossRef]
32. Tichadou, L.; Glaizal, M.; Armengaud, A.; Grossel, H.; Lemée, R.; Kantin, R.; Lasalle, J.L.; Drouet, G.; Rambaud, L.; Malfait, P.; et al. Health Impact of unicellular algae of the *Ostreopsis* genus blooms in the Mediterranean Sea: Experience of the French Mediterranean coast surveillance network from 2006 to 2009. *Clin. Toxicol.* **2010**, *48*, 839–844. [CrossRef] [PubMed]
33. Vila, M.; Abós-Herràndiz, R.; Isern-Fontanet, J.; Àlvarez, J.; Berdalet, E. Establishing the link between *Ostreopsis* cf. *ovata* blooms and human health impacts using ecology and epidemiology. *Sci. Mar.* **2016**, *80*, 107–115. [CrossRef]
34. Gallitelli, M.; Ungaro, N.; Addante, L.M.; Silver, N.G.; Sabba, C. Respiratory illness as a reaction to tropical algal blooms occurring in a temperate climate. *JAMA-J. Am. Med. Assoc.* **2005**, *293*, 2599–2600.
35. Biré, R.; Trotereau, S.; Lemée, R.; Delpont, C.; Chabot, B.; Aumond, Y.; Krys, S. Occurrence of palytoxins in marine organisms from different trophic levels of the French Mediterranean coast harvested in 2009. *Harmful Algae* **2013**, *28*, 10–22. [CrossRef]
36. Gleibs, S.; Mebs, D. Distribution and sequestration of palytoxin in coral reef animals. *Toxicon* **1999**, *37*, 1521–1527. [CrossRef]
37. Sansoni, G.; Borghini, B.; Camici, G.; Casotti, M.; Righini, P.; Rustighi, C. Fioriture algali di *Ostreopsis ovata* (Gonyaulacales: Dinophyceae): Un problema emergente. *Biol. Ambient.* **2003**, *17*, 17–23.
38. Ferreira, C.E.L. Sea urchins killed by toxic algae. *J. Mar. Biol. Assoc. Glob. Mar. Environ.* **2006**, *3*, 22–23.
39. Shears, N.T.; Ross, P.M. Blooms of benthic dinoflagellates of the genus *Ostreopsis*; an increasing and ecologically important phenomenon on temperate reefs in New Zealand and worldwide. *Harmful Algae* **2009**, *8*, 916–925. [CrossRef]
40. Giussani, V.; Costa, E.; Pecorino, D.; Berdalet, E.; De Giampaulis, G.; Gentile, M.; Fuentes, V.; Vila, M.; Penna, A.; Chiantore, M.; et al. Effects of the harmful dinoflagellate *Ostreopsis* cf. *ovata* on different life cycle stages of the common moon jellyfish *Aurelia* sp. *Harmful Algae* **2016**, *57*, 49–58. [CrossRef]
41. Simonini, R.; Orlandi, M.; Abbate, M. Is the toxic dinoflagellate *Ostreopsis* cf. *ovata* harmful to Mediterranean benthic invertebrates? Evidences from ecotoxicological tests with the polychaete *Dinophilus gyrociliatus*. *Mar. Environ. Res.* **2011**, *72*, 230–233. [CrossRef]
42. Faimali, M.; Giussani, V.; Piazza, V.; Garaventa, F.; Corrà, C.; Asnaghi, V.; Privitera, D.; Gallus, L.; Cattaneo-Vietti, R.; Mangialajo, L.; et al. Toxic effects of harmful benthic dinoflagellate *Ostreopsis ovata* on invertebrate and vertebrate marine organisms. *Mar. Environ. Res.* **2012**, *76*, 97–107. [CrossRef] [PubMed]
43. Pagliara, P.; Caroppo, C. Toxicity assessment of *Amphidinium carterae*, *Coolia* cfr. *monotis* and *Ostreopsis* cfr. *ovata* (Dinophyta) isolated from the northern Ionian Sea (Mediterranean Sea). *Toxicon* **2012**, *60*, 1203–1214. [CrossRef] [PubMed]
44. Migliaccio, O.; Castellano, I.; Di Cioccio, D.; Tedeschi, G.; Negri, A.; Cirino, P.; Romano, G.; Zingone, A.; Palumbo, A. Subtle reproductive impairment through nitric oxide-mediated mechanisms in sea urchins from an area affected by harmful algal blooms. *Sci. Rep.* **2016**, *6*, 26086. [CrossRef] [PubMed]
45. Neves, R.A.F.; Contins, M.; Nascimento, S.M. Effects of the toxic benthic dinoflagellate *Ostreopsis* cf. *ovata* on fertilization and early development of the sea urchin *Lytechinus variegatus*. *Mar. Environ. Res.* **2018**, *135*, 11–17. [CrossRef]

46. Louzao, M.C.; Espiña, B.; Cagide, E.; Ares, I.R.; Alfonso, A.; Vieytes, M.R.; Botana, L.M. Cytotoxic effect of palytoxin on mussel. *Toxicon* **2010**, *56*, 842–847. [CrossRef]
47. Malagoli, D.; Casarini, L.; Ottaviani, E. Effects of the marine toxins okadaic acid and palytoxin on mussel phagocytosis. *Fish Shellfish Immunol.* **2008**, *24*, 180–186. [CrossRef]
48. Gorbi, S.; Bocchetti, R.; Binelli, A.; Bacchiocchi, S.; Orletti, R.; Nanetti, L.; Raffaelli, F.; Vignini, A.; Accoroni, S.; Totti, C.; et al. Biological effects of palytoxin-like compounds from *Ostreopsis* cf. *ovata*: A multibiomarkers approach with mussels *Mytilus galloprovincialis*. *Chemosphere* **2012**, *89*, 623–632. [CrossRef]
49. Gorbi, S.; Avio, G.C.; Benedetti, M.; Totti, C.; Accoroni, S.; Pichierri, S.; Bacchiocchi, S.; Orletti, R.; Graziosi, T.; Regoli, F. Effects of harmful dinoflagellate *Ostreopsis* cf. *ovata* exposure on immunological, histological and oxidative responses of mussels *Mytilus galloprovincialis*. *Fish Shellfish Immunol.* **2013**, *35*, 941–950. [CrossRef]
50. Carella, F.; Sardo, A.; Mangoni, O.; Di Cioccio, D.; Urciuolo, G.; De Vico, G.; Zingone, A. Quantitative histopathology of the Mediterranean mussel (*Mytilus galloprovincialis* L.) exposed to the harmful dinoflagellate *Ostreopsis* cf. *ovata*. *J. Invertebr. Pathol.* **2015**, *127*, 130–140. [CrossRef]
51. Sardo, A.; Rossi, R.; Soprano, V.; Ciminiello, P.; Fattorusso, E.; Cirino, P.; Zingone, A. The dual impact of *Ostreopsis* cf. *ovata* on *Mytilus galloprovincialis* and *Paracentrotus lividus*: Toxin accumulation and pathological aspects. *Mediterr. Mar. Sci.* **2020**, *22*, 59–72. [CrossRef]
52. Aligizaki, K.; Nikolaidis, G. Morphological identification of two tropical dinoflagellates of the genera *Gambierdiscus* and *Sinophysis* in the Mediterranean Sea. *J. Biol. Res.* **2008**, *9*, 75–82.
53. Amzil, Z.; Sibat, M.; Chomerat, N.; Grossel, H.; Marco-Miralles, F.; Lemee, R.; Nezan, E.; Sechet, V. Ovatoxin-a and palytoxin accumulation in seafood in relation to *Ostreopsis* cf. *ovata* blooms on the French Mediterranean coast. *Mar. Drugs* **2012**, *10*, 477–496. [CrossRef] [PubMed]
54. Accoroni, S.; Romagnoli, T.; Colombo, F.; Pennesi, C.; di Camillo, C.G.; Marini, M.; Battocchi, C.; Ciminiello, P.; Dell'Aversano, C.; Dello Iacovo, E.; et al. *Ostreopsis* cf. *ovata* bloom in the northern Adriatic Sea during summer 2009: Ecology, molecular characterization and toxin profile. *Mar. Pollut. Bull.* **2011**, *62*, 2512–2519. [CrossRef] [PubMed]
55. EFSA Scientific Opinion on marine biotoxins in shellfish—Palytoxin group. *EFSA J.* **2009**, *7*, 1393. [CrossRef]
56. Totti, C.; Accoroni, S.; Cerino, F.; Cucchiari, E.; Romagnoli, T. *Ostreopsis ovata* bloom along the Conero Riviera (northern Adriatic Sea): Relationships with environmental conditions and substrata. *Harmful Algae* **2010**, *9*, 233–239. [CrossRef]
57. Throndsen, J. Preservation and storage. In *Phytoplankton Manual*; Sournia, A., Ed.; UNESCO: Paris, France, 1978; Volume 6, pp. 69–74.
58. Hasle, G.R. The inverted microscope method. In *Phytoplankton Manual*; Sournia, A., Ed.; UNESCO: Paris, France, 1978; Volume 6, pp. 88–96.
59. Hoshaw, R.W.; Rosowski, J.R. Methods for microscopic algae. In *Handbook of Phycological Methods*; Stein, J.R., Ed.; Cambridge University Press: New York, NY, USA, 1973; pp. 53–67.
60. Guillard, R.R.L. Culture of phytoplankton for feeding marine invertebrates. In *Culture of Marine Invertebrate Animals*; Smith, W.L., Chanley, M.H., Eds.; Plenum Press: New York, NY, USA, 1975; pp. 26–60.
61. Doyle, J.J.; Doyle, J.L. A Rapid DNA isolation procedure for small quantities of fresh leaf tissue. *Phytochem. Bull.* **1987**, *19*, 11–15.
62. Accoroni, S.; Giulietti, S.; Romagnoli, T.; Siracusa, M.; Bacchiocchi, S.; Totti, C. Morphological variability of *Pseudo-nitzschia pungens* clade I (Bacillariophyceae) in the northwestern Adriatic Sea. *Plants* **2020**, *9*, 1420. [CrossRef]
63. Scholin, C.A.; Herzog, M.; Sogin, M.; Anderson, D.M. Identification of group and strain-specific genetic markers for globally distributed *Alexandrium* (Dinophyceae). II. Sequence analysis of a fragment of the LSU rRNA gene. *J Phycol.* **1994**, *30*, 999–1011. [CrossRef]
64. Ciminiello, P.; Dell'Aversano, C.; Dello Iacovo, E.; Fattorusso, E.; Forino, M.; Tartaglione, L.; Rossi, R.; Soprano, V.; Capozzo, D.; Serpe, L. Palytoxin in seafood by liquid chromatography tandem mass spectrometry: Investigation of extraction efficiency and matrix effect. *Anal. Bioanal. Chem.* **2011**, *401*, 1043–1050. [CrossRef]
65. Strickland, J.D.H.; Parsons, T.R. *A practical handbook of seawater analysis, Bulletin 167*, 2nd ed.; Printing and Publishing Supply and Services Canada: Ottawa, ON, Canada, 1972; pp. 1–310.
66. Accoroni, S.; Glibert, P.M.; Pichierri, S.; Romagnoli, T.; Marini, M.; Totti, C. A conceptual model of annual *Ostreopsis* cf. ovata blooms in the northern Adriatic Sea based on the synergic effects of hydrodynamics, temperature, and the N:P ratio of water column nutrients. *Harmful Algae* **2015**, *45*, 14–25. [CrossRef]
67. Accoroni, S.; Colombo, F.; Pichierri, S.; Romagnoli, T.; Marini, M.; Battocchi, C.; Penna, A.; Totti, C. Ecology of *Ostreopsis* cf. *ovata* blooms in the northwestern Adriatic Sea. *Cryptogam. Algol.* **2012**, *33*, 191–198. [CrossRef]
68. Accoroni, S.; Tartaglione, L.; Dello Iacovo, E.; Pichierri, S.; Marini, M.; Campanelli, A.; Dell'Aversano, C.; Totti, C. Influence of environmental factors on the toxin production of *Ostreopsis* cf. *ovata* during bloom events. *Mar. Pollut. Bull.* **2017**, *123*, 261–268. [CrossRef] [PubMed]
69. Tartaglione, L.; Dello Iacovo, E.; Mazzeo, A.; Casabianca, S.; Ciminiello, P.; Penna, A.; Dell'Aversano, C. Variability in toxin profiles of the Mediterranean *Ostreopsis* cf. *ovata* and in structural features of the produced ovatoxins. *Environ. Sci. Technol.* **2017**, *51*, 13920–13928. [CrossRef] [PubMed]
70. Reis Costa, P.; Braga, A.; Turner, A. Accumulation and elimination dynamics of the hydroxybenzoate saxitoxin analogues in mussels *Mytilus galloprovincialis* exposed to the toxic marine dinoflagellate *Gymnodinium catenatum*. *Toxins* **2018**, *10*, 428. [CrossRef] [PubMed]
71. Blanco, J. Accumulation of *Dinophysis* toxins in bivalve molluscs. *Toxins* **2018**, *10*, 453. [CrossRef] [PubMed]

72. Jauffrais, T.; Marcaillou, C.; Herrenknecht, C.; Truquet, P.; Sechet, V.; Nicolau, E.; Tillmann, U.; Hess, P. Azaspiracid accumulation, detoxification and biotransformation in blue mussels (*Mytilus edulis*) experimentally fed *Azadinium spinosum*. *Toxicon* **2012**, *60*, 582–595. [CrossRef] [PubMed]
73. Giuliani, M.E.; Accoroni, S.; Mezzelani, M.; Lugarini, F.; Bacchiocchi, S.; Siracusa, M.; Tavoloni, T.; Piersanti, A.; Totti, C.; Regoli, F.; et al. Biological effects of the azaspiracid-producing dinoflagellate *Azadinium dexteroporum* in *Mytilus galloprovincialis* from the Mediterranean Sea. *Mar. Drugs* **2019**, *17*, 595. [CrossRef]
74. Lin, C.; Accoroni, S.; Glibert, P. *Karlodinium veneficum* feeding responses and effects on larvae of the eastern oyster *Crassostrea virginica* under variable nitrogen:phosphorus stoichiometry. *Aquat. Microb. Ecol.* **2017**, *79*, 101–114. [CrossRef]
75. Gémin, M.-P.; Réveillon, D.; Hervé, F.; Pavaux, A.-S.; Tharaud, M.; Séchet, V.; Bertrand, S.; Lemée, R.; Amzil, Z. Toxin content of *Ostreopsis* cf. *ovata* depends on bloom phases, depth and macroalgal substrate in the NW Mediterranean Sea. *Harmful Algae* **2020**, *92*, 101727. [CrossRef]
76. Andersen, P. *Monitoring Toxic Algae in Relation to the Danish Mussel Fisheries 1991–1997*; Technical Report for The Danish Veterinary and Food Administration: Frederiksberg, Denmark, 1998; pp. 1–19.
77. Reguera, B.; Riobó, P.; Rodríguez, F.; Díaz, P.A.; Pizarro, G.; Paz, B.; Franco, J.M.; Blanco, J. *Dinophysis* toxins: Causative organisms, distribution and fate in shellfish. *Mar. Drugs* **2014**, *12*, 394–461. [CrossRef]
78. Landsberg, J.H. The effects of harmful algal blooms on aquatic organisms. *Rev. Fish. Sci.* **2002**, *10*, 113–390. [CrossRef]
79. Bricelj, V.M.; Shumway, S.E. Paralytic shellfish toxins in bivalve molluscs: Occurrence, transfer kinetics, and biotransformation. *Rev. Fish. Sci.* **1998**, *6*, 315–383. [CrossRef]
80. Accoroni, S.; Totti, C.; Razza, E.; Congestri, R.; Campanelli, A.; Marini, M.; Ellwood, N.T.W. Phosphatase activities of a microepiphytic community during a bloom of *Ostreopsis* cf. *ovata* in the northern Adriatic Sea. *Water Res.* **2017**, *120*, 272–279. [CrossRef] [PubMed]
81. Chang, F.H.; Shimizu, Y.; Hay, B.; Stewart, R.; Mackay, G.; Tasker, R. Three recently recorded *Ostreopsis* spp. (Dinophyceae) in New Zealand: Temporal and regional distribution in the upper North Island from 1995 to 1997. *N. Z. J. Mar. Freshw. Res.* **2000**, *34*, 29–39. [CrossRef]
82. Selina, M.S.; Morozova, T.V.; Vyshkvartsev, D.I.; Orlova, T.Y. Seasonal dynamics and spatial distribution of epiphytic dinoflagellates in Peter the Great Bay (Sea of Japan) with Special emphasis on *Ostreopsis* species. *Harmful Algae* **2014**, *32*, 1–10. [CrossRef]
83. Mabrouk, L.; Hamza, A.; Brahim, M.B.; Bradai, M.N. Temporal and depth distribution of microepiphytes on *Posidonia oceanica* (L.) Delile leaves in a meadow off Tunisia. *Mar. Ecol.* **2011**, *32*, 148–161. [CrossRef]
84. Funari, E.; Manganelli, M.; Testai, E. *Ostreospis* cf. *ovata* blooms in coastal water: Italian guidelines to assess and manage the risk associated to bathing waters and recreational activities. *Harmful Algae* **2015**, *50*, 45–56. [CrossRef]